Pergamon

Cement and Concrete Research 30 (2000) 809–816

CEMENT AND CONCRETE RESEARCH

A unique experimental method for monitoring aggregate settlement in concrete

Michael F. Petrou[a], Kent A. Harries[a,*], Francis Gadala-Maria[b], Venkata Giri Kolli[b]

[a]*Department of Civil and Environmental Engineering, University of South Carolina, 300 Main Street, Columbia, SC 29208, USA*
[b]*Department of Chemical Engineering, University of South Carolina, Columbia, SC 29208, USA*

Received 17 November 1999; accepted 28 January 2000

Abstract

A unique experimental method for monitoring the settlement of aggregate in fresh concrete is introduced and demonstrated. Using nuclear medicine techniques, real-time images of aggregate settlement due to vibration are obtained. These images are used to study the rheological properties of the vibrated concrete mix. The technique developed allows the experimental verification of a number of assumptions regarding the rheology of fresh concrete and the implications of the accepted rheological model of fresh concrete. Additionally, the effects of vibration on aggregate settlement are clearly shown, including effects resulting from the location of the vibrator and the size and density of the aggregate.

Keywords: Fresh concrete; Rheology; Vibration; Modeling; Radioisotope imaging

1. Introduction

Fresh concrete is a multi-component mixture consisting of cement, water, sand, coarse aggregate, and additives such as superplasticizers, silica fume, and fly ash. When water is added to the mixture of solids, it becomes a "plastic" concrete mix, which over time sets and becomes a hard, rock-like material due to the hydration reactions that take place in the concrete [1]. During its plastic stage, it is generally believed that heavier coarse aggregate settles down while the lighter elements such as entrapped air, water, and mortar are pushed upward, resulting in certain undesirable effects such as "bleeding" and a weakening of the bond between reinforcing bars and concrete. This last phenomenon is called the "top bar effect" since it is most noticeable in the bars nearest the top of the section and is known to significantly affect the structural behavior of concrete elements. Recently, the "top bar effect" has been identified as being critical in the poor performance of precast concrete piles [2]. It is this connection that has led the authors to seek a more fundamental understanding of the properties of fresh concrete in order to explain and provide guidance to mitigate this effect.

Fresh concrete exhibits a yield stress below which it behaves as a solid, and above which it flows as a liquid [3]. The presence of a yield stress in a medium retards, and may even prevent, the natural settlement of heavier solids in it [4]. A solid may or may not sink in a medium depending on the size of the solid, the magnitude of the yield stress of the medium, and the density difference between the solid and the medium. During placement and compaction, fresh concrete is usually vibrated or tapped to make it flow more easily. Under vibration, there is a significant reduction in the yield stress [5–7] and a decrease in the viscosity [5] of the concrete. It is not clear whether coarse aggregate settles in concrete only during placement or also after placement. Also, during placement, it is not clear whether the coarse aggregate settles all the time or only during vibration. Therefore, there is a need to understand the influence of the rheology of concrete and the placement procedures, in particular the effect of vibration, on aggregate settlement.

1.1. Rheology of fresh concrete

The rheology of fresh concrete is complex due to its composition and the accompanying changes of properties

* Corresponding author. Tel.: +1-803-777-0671; fax: +1-803-777-0670.
E-mail address: harries@engr.sc.edu (K.A. Harries).

0008-8846/00/$ – see front matter
PII: S0008-8846(00)00223-4

with respect to time. Previous researchers have described fresh concrete as a complex non-Newtonian material that possesses a yield stress and a shear-rate dependent viscosity. Both the yield stress and the viscosity change with time [6–10]. As the concrete sets, the yield stress and the viscosity increase greatly. In practice, the flow behavior of fresh concrete is simply represented by the Bingham model [3,11,12]:

$$\tau = \tau_0 + \eta_p \dot{\gamma} \quad (1)$$

where τ is the shear stress, τ_0 is the yield stress, $\dot{\gamma}$ is strain rate (or shear rate), and η_p is the plastic viscosity.

When fresh concrete is subjected to vibration, previous researchers have observed significant changes in its rheological properties. Using an apparatus described as a "two-point workability apparatus," Tattersall et al. [5,6] concluded that concrete under vibration loses its yield stress. Using a similar apparatus, Kakuta and Kojima [8] determined that concrete under vibration changes from a thixotropic material with a yield stress to an apparently non-thixotropic, shear-thinning material with little or no yield stress. de Larrard et al. [7], using a BTRHEOM apparatus fitted with grooved parallel plates, found that under vibration, the yield stress of the concrete mixtures used in their studies decreased to half its magnitude and in some cases, became negligible.

With regards to the viscosity, some researchers have found that under vibration, the plastic viscosity, η_p, of concrete changes and the concrete becomes shear-thinning [5,6,8]. However, de Larrard et al. [7] found the plastic viscosity to be unaffected by vibration. Even if the plastic viscosity does not decrease under vibration, the concrete would still become more workable because of the decrease in the yield stress. This is because the viscosity is the ratio of shear stress to shear rate.

The presence of a yield stress in concrete mixtures has not been explained in terms of their microstructure, and only recently has there been some work in that direction. The concentration of solids in concrete is very high. The size of these solid particles varies anywhere from a fraction of a micron to a few centimeters, and the morphology of these particles also varies. The yield stress of concrete mixtures may have three primary contributing sources. One source is the mechanical interlocking of the larger, irregularly shaped, rough aggregate which form the basic skeleton of the concrete matrix [10]. The second source of yield stress may be the attractive colloidal forces between the cement and other sub-micron particles that cause them to flocculate [13]. The third source, which contributes to the ultimate hardening of the concrete mixtures and cements, is a colloidal gel of hydrated calcium silicate that forms around the cement particles as a result of the reaction between cement and water [1].

The causes of the decrease in yield stress due to vibration are not understood either. It is speculated that vibration deflocculates the cement aggregate and also breaks the initially weak chemical bonds resulting from gelation in fresh cement paste. The vibration may also cause the larger aggregate to "jiggle," thus unlocking the initially interlocked matrix. Therefore, the reduction in the yield stress of concrete mixtures under vibration may be related to the weakening of the mechanical and chemical bonds among its ingredients.

1.2. Criteria for aggregate settlement in fresh concrete

A solid sphere submerged in a Newtonian fluid (zero yield stress) with a density lower than that of the sphere sinks in the fluid with a terminal velocity U_t, which may be derived from the Stokes drag to be [Eq. (2)]:

$$U_t = \frac{2}{9}\frac{R^2(\rho_s - \rho_f)g}{\mu} \quad (2)$$

where R is the radius of the sphere, ρ_s is the density of the sphere, ρ_f is the density of the fluid, g is the acceleration due to gravity, and μ is the viscosity of the fluid.

If the fluid possesses a yield stress, however, the sphere may not sink at all even if its density is greater than the density of the fluid. Beris et al. [4] have predicted that a spherical particle will settle in a fluid having Bingham plastic behavior (non-zero yield stress) only when the dimensionless group referred to as the yield stress parameter Y_g, defined below, is less than 0.143.

$$Y_g = \frac{3\tau_0}{2R(\rho_s - \rho_f)g.} \quad (3)$$

Since unvibrated concrete possesses a significant yield stress, typically-sized aggregate will not settle without a significant reduction in the yield stress. Petrou et al. [14] have conducted experiments demonstrating that even very large aggregate (up to about half a meter across) does not settle in a standard mortar mix without vibration.

1.3. Prediction of aggregate settlement in fresh concrete

The authors propose predicting the settlement of aggregate by applying rheological equations for the motion of a sphere in a Bingham plastic fluid. Beris et al. [4] propose a set of equations relating the Stokes drag coefficient,

$$C_S = \frac{2R^2(\rho_s - \rho_f)g}{9\eta_p U_t} \quad (4)$$

and the Bingham number, N_B, a dimensionless parameter which is a measure of the ratio of the yield stress to the viscous stress, defined as:

$$N_B = \frac{2\tau_0 R}{\eta_p U_t.} \quad (5)$$

If settlement of aggregate occurs, an upper bound of the fluid yield stress, τ_0, may be estimated from Eq. (3). The settling velocity, U_t, or plastic viscosity, η_p, may be com-

puted, knowing the other, from the following asymptotic relationships [4]:

$$\ln(C_S - 1) = 0.91 + 0.55\ \ln N_B \text{ for } 0.005 \le N_B \le 0.012, \quad (6)$$

$$C_S = 1 + 1.874\ N_B^{1/2} + 1.152\ N_B \text{ for } 0.012 \le N_B \le 600,$$

and

$$C_S = \frac{1.031 Y_g}{(Y_{gl} - Y_g)^2} \text{ for } N_B \ge 600$$

where $Y_{gl} = 0.143$ is the limiting value for the yield stress parameter Y_g given in Eq. (3). It is noted that the Stokes drag coefficient, C_S, is equal to unity for spheres falling in Newtonian fluids.

The equations presented assume a spherical aggregate. For non-spherical aggregate, the radius, R, may be replaced with the hydraulic radius, R_h [Eq. (7)]:

$$R_h = \left(\frac{m/\rho_s}{\frac{4}{3}\pi} \right)^{1/3} \quad (7)$$

where m and ρ_s are the mass and density of the aggregate, respectively.

1.4. Modeling aggregate settlement

Aggregate settlement in mortar was modeled by Petrou et al. [14] as spheres settling in a Bingham plastic. It was predicted that typically-sized aggregate does not settle in mortar nor, consequently, in concrete. This was confirmed experimentally. Nonetheless, it was also found that when subjected to vibration, the mortar loses most if not all of its yield stress and that aggregate settles in mortar. It is therefore important to understand how vibration affects the rheology of concrete in order to be able to model the settlement of aggregate. It is noted that most preliminary modeling uses mortar, rather than concrete, since it is more homogeneous. It is generally assumed that concrete will have a greater yield stress and viscosity than mortar.

By modeling settlement of aggregate in mortar as settlement of a single sphere in a large pool of Bingham plastic, it is feasible to predict settlement in a particular period of time. It is not so simple, however, to obtain the Bingham parameters (yield stress and plastic viscosity) that characterize the mortar under vibration since the effect of vibration is not uniform throughout the fresh mortar. The mortar closest to the vibrator is affected the most. In addition, it is possible that the effect of vibration is different at different depths. Modeling efforts are further complicated by the fact that the rheological properties depend on many additional factors including the composition of concrete or mortar, the age of the concrete or mortar, the type of vibration applied (frequency, amplitude, geometry of the vibrator, etc.), the manner in which the vibration is applied (to the form or inside the concrete), the position of the aggregate relative to the vibrator, and the duration of vibration.

In order to monitor the aggregate settlement and to investigate these parameters, an experimental technique used in nuclear medicine was adapted.

2. Unique experimental method

The objective of the unique experimental method introduced here is to develop a procedure to monitor aggregate settlement in concrete in real-time and to investigate the rheological properties of concrete. A scintillation camera is utilized to observe and record settlement of radioactively "tagged" aggregate in mortar and concrete in real-time. The captured real-time images are analyzed to experimentally determine the rheological properties of concrete or mortar.

The experimental procedure demonstrated here uses metallic spheres as tagged aggregate. The use of spheres simplifies the rheological equations by eliminating the need to determine the effect of aggregate shape and orientation. Aluminum spheres were selected to represent aggregate since the specific gravity of aluminum (2.70) is similar to that of typical stone aggregate. For comparison and in order to verify and calibrate the rheological equations, steel spheres having a specific gravity of 7.75 were also used in some experiments. Only the few tagged aggregates in each experiment are metallic spheres. The

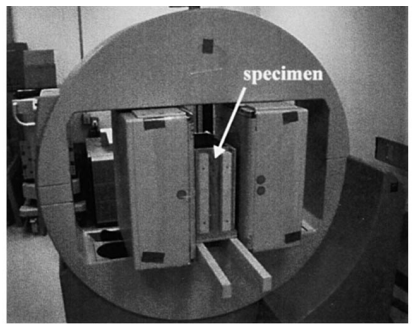

(a) scintillation camera and pilot test specimen

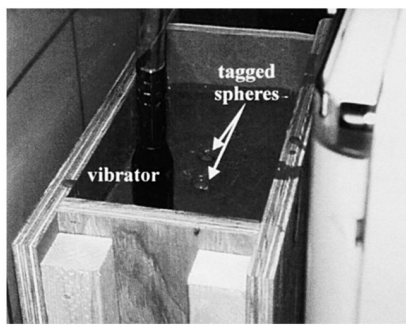

(b) specimen showing vibrator and two "tagged" spheres

Fig. 1. Test setup.

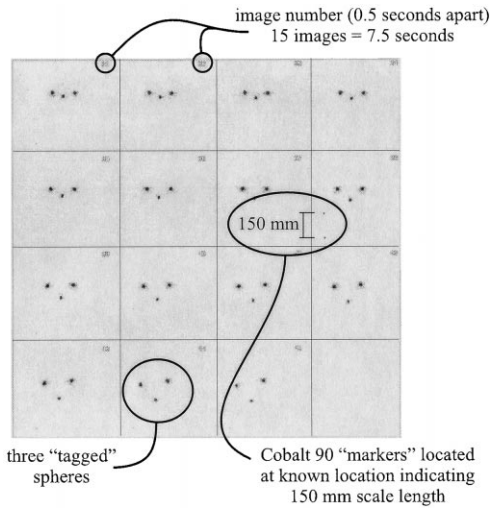

Fig. 2. Sample image sequence (from test 2) from scintillation camera showing 7.5-s time span during vibration.

concrete mixes used for the experiment use typically available stone aggregate.

In order to tag the spheres, a 3-mm hole was drilled just beyond the center of the sphere. Into this hole, a solution of technetium 99 isotope was placed and the hole was sealed with fast-drying water-proof epoxy. Technetium 99 emits gamma particles at 140 keV and has a half-life of approximately 6 h. Once tagged, the spheres are easily detected by the scintillation camera for at least 6 h, giving the investigators ample time to conduct a series of settlement tests.

The settlement tests were conducted in forms 300-mm^2 by 150-mm thick. The concrete or mortar was placed in the forms and the forms were immediately placed on the bed of the scintillation camera. Fig. 1a shows the forms in the scintillation camera. The tagged spheres were then introduced to the surface of the concrete or mortar at locations appropriate for the test being conducted (see Fig. 1b).

The scintillation camera has a viewing area of approximately 400 mm^2; thus, the entire specimen is visible to the camera. The scintillation camera consists of an array of receptors tuned to 140 keV, the energy level of the technetium 99 isotope. The images produced show the tagged aggregate very clearly. Imaging software filters out other energy levels resulting in an exceptionally clear image. An example of the output generated is shown in Fig. 2. This output screen shows a sequence of images, 0.5 s apart, arranged in chronological order from the top left. The images show three tagged spheres settling in mortar subject to vibration (the vibration was started just before this sequence begins). In this sequence, the middle sphere (steel) is settling faster than the others (aluminum) on either side of it. Additionally, the aluminum sphere closest to the vibrator settles faster than the one farthest away.

The scintillation camera may be programmed to take a snapshot of the specimen at any time interval desired. The resulting output is therefore a series of images recorded at a particular time step. For the initial studies, a time step of 0.5 s was found to be sufficient to generate a "real-time" recording of the aggregate settlement. Due to hardware processing speed, it is unlikely that a smaller time step is practical, nor is it considered necessary.

The test protocol varied somewhat from specimen to specimen but followed the same general sequence:

1. Testing began 5 min after the concrete or mortar was placed in the form.
2. The scintillation camera recorded a few images during the time the specimen remained undisturbed.
3. The specimen was vibrated for 15 s during which time the scintillation camera recorded images every 0.5 s.
4. Vibration was stopped and the camera continued to record images for a period of time after this.

Although not investigated here, it is possible to repeat this sequence after a fixed length of time in order to investigate the effects of re-vibration. Continued repetition is possible until "first set" of the concrete or mortar.

After testing, the recorded images are digitized and may be manipulated by any graphics-handling program. Cobalt 90 reference markers are used to provide a frame of reference and a scale as shown in Figs. 2 and 3. Using the established frame of reference, spatial displacements may be easily determined from each image. Displacement data obtained from a series of images allows the velocity

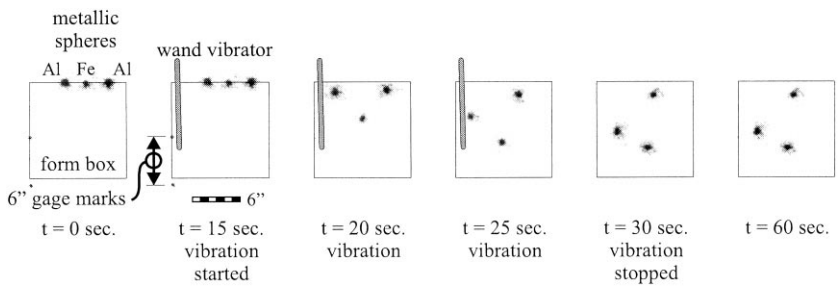

Fig. 3. Series of images from test 2.

of the tagged aggregate to be determined. An example of a series of images from this study is shown in Fig. 3.

3. Experimental results

To demonstrate the experimental method described, an initial study was conducted. Two mortar specimens (tests 1 and 2) and a concrete specimen (test 3) were prepared. Steel (Fe) spheres 19 mm in diameter and aluminum (Al) spheres 22 mm in diameter were tagged and introduced into the specimens (see Fig. 1b). Table 1 gives the mortar and concrete mix designs and test parameters for each of the tests.

The concrete vibrator used for the tests had a 35-mm diameter tip and a vibration speed of 10 000 rpm. The vibrator was inserted into the forms about 50 mm from one end (see Fig. 1b). The vibrator tip was not allowed to come into contact with the forms at any time.

A sequence of images (from test 2), taken 0.5 s apart is shown in Fig. 2. All recorded images were digitized. The locations of the tagged aggregate were determined using a cross-hair pointer aligned with the center of the circular region of emissions representing the aggregate. There is a small operator-introduced error associated with this method resulting from the irregular tagged images. For this reason, the same operator analyzed all images minimizing interpretation error. It is estimated that using this method the aggregate may be located with a precision of about ±2 mm or about 1.3% of the entire specimen dimension. In the future, computerized digitizing capabilities will be added to the scintillation camera being used.

Fig. 3 shows a sample sequence (from test 2) of aggregate settling in mortar. The vibrator and form outlines are not picked up by the detector and have been drawn in the images for reference only. Three tagged spheres are shown. As is discussed below, it can be seen that the middle steel sphere (Fe) is settling faster than the outer aluminum (Al) spheres. Additionally, it can be seen that the spheres closer to the vibrator settle at a faster rate and that the settlement stops when the vibration stops. These observations are discussed below.

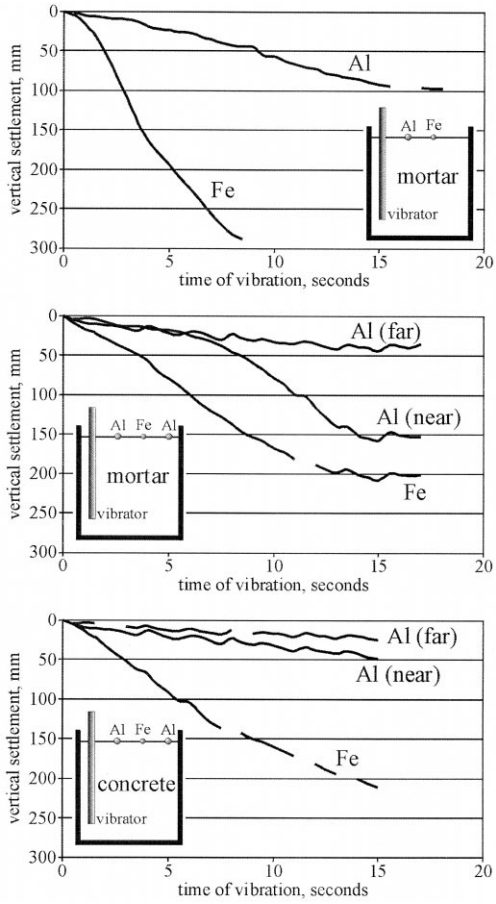

Fig. 4. Experimental settlement vs. time plots.

Table 1
Mix designs and test parameters

	Test 1 (Mortar 1)	Test 2 (Mortar 2)	Test 3 (Concrete)
Mix design			
Type 1 cement	15.3 kg	9.1 kg	13.4 kg
Water	7.6 kg	4.5 kg	8.3 kg
Sand	19.1 kg	27.3 kg	26.7 kg
3/8 in. Aggregate	none	none	13.0 kg
#4 Aggregate	none	none	9.1 kg
#8 Aggregate	none	none	4.5 kg
Admixtures	none	none	none
Water:cement ratio	0.50	0.50	0.62
Test parameters			
Time elapsed from placement to vibration (min)	5	7	7
Duration of vibration (s)	18.5	17	15
Location of tagged spheres relative to vibrator	Al @ 75 mm Fe @ 150 mm	Al @ 75 mm Fe @ 150 mm Al @ 225 mm	Al @ 75 mm Fe @ 150 mm Al @ 225 mm

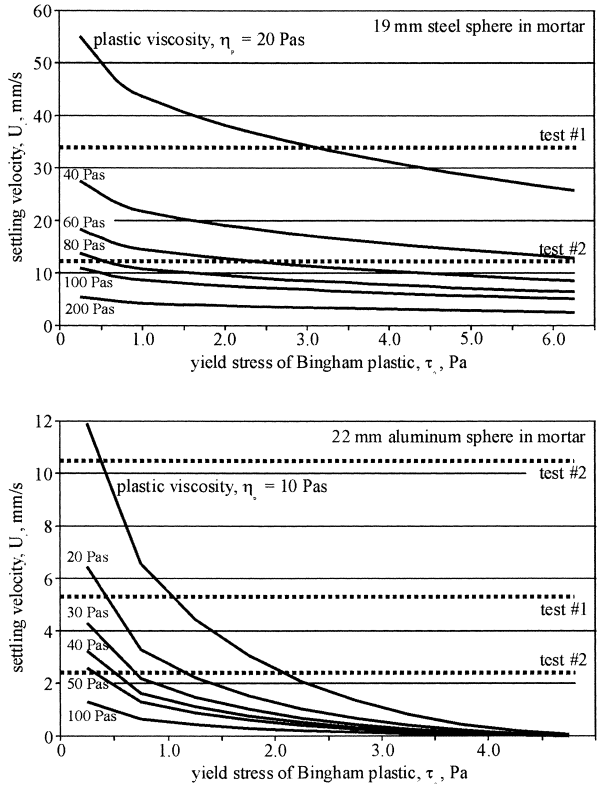

Fig. 5. Settlement predictions for mortar.

Fig. 4 shows plots of the experimentally observed vertical settlement vs. time for the three tests. The slope of these plots is equal to the vertical velocity of the settling aggregate.

3.1. Experimental observations and discussion of results

The following observations regarding the settlement of spheres in mortar or concrete were made.

(1) Prior to vibration and after the cessation of vibration, there was no noticeable settlement. This observation is consistent with predictions and previous experimental results reported above.

(2) As can be seen from the slopes of the settlement curves shown in Fig. 4, once vibration begins, the spheres rapidly reached their terminal velocities. This is an indication that the rheological properties change from their unvibrated to their vibrated values almost instantly. Settlement stopped as soon as vibration was terminated.

(3) The denser steel sphere settled notably faster than the aluminum spheres even though it was smaller. This observation is predicted by the equations reported above. Based on these equations, the steel spheres should settle with a velocity 8.5 times greater than the aluminum spheres if all other parameters are equal.

(4) By comparing the settlement of the identical aluminum spheres in tests 2 and 3, a spatial effect was observed. Spheres further form the vibrator settled at a significantly slower rate. This observation is consistent with the fact that the effectiveness of vibration dissipates with distance from the vibrator. Vibration had a noticeable effect on aggregate settlement at a distance of at least in a 225 mm.

(5) Although barely perceptible in Figs. 2 and 3, there was an observed tendency of the spheres to migrate horizontally toward the vibrator while settling vertically. This effect is more pronounced closer to the vibrator. The cause of this horizontal migration is unclear although it may be due to the gradient of viscosity with distance from the vibrator or it may be an indication of a secondary flow caused by the shape of the form or location of the vibrator in the form.

4. Comparison of experimental and predicted settlements

Predictions of aggregate settlement were made for the test specimens using Eqs. (4)–(6). The resulting settling velocity vs. yield stress plots for different plastic viscosity values are shown in Figs. 5 and 6 for mortar and concrete, respectively. In order to develop these curves, the density of mortar was assumed to be 2170 kg/m^3 and the density of the concrete was assumed to be 2240 kg/m^3. Also shown, as the

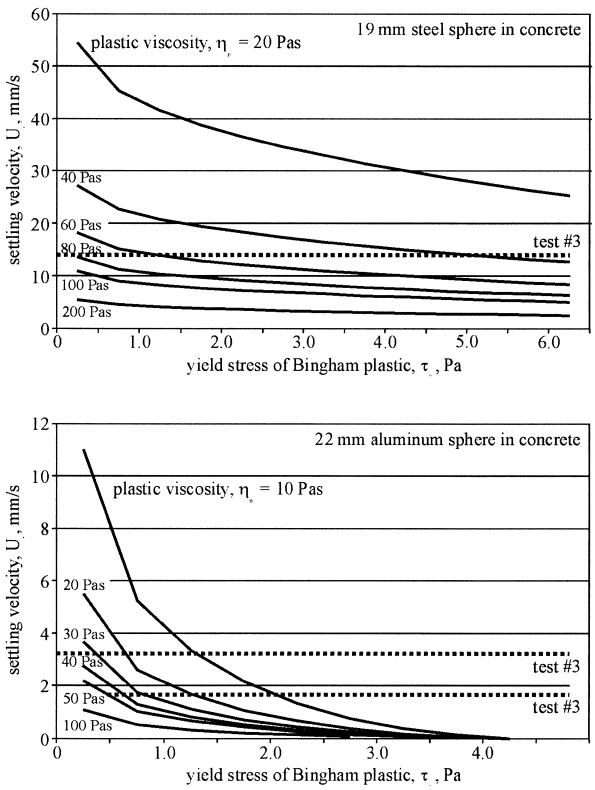

Fig. 6. Settlement predictions for concrete.

Table 2
Experimental results

	Test 1 (Mortar 1)	Test 2 (Mortar 2)	Test 3 (Concrete)
Settlement of 22 mm Al @ 75 mm	94	156	48
Time (s)	18.5	17	15
Average velocity (mm/s)	5.1	9.2	3.2
Viscosity calculated from Eq. (1) (Pa s)	25.4	14.1	34.6
Settlement of 19 mm Fe @ 150 mm	289	201	211
Time (s)	8.5	17	15
Average velocity (mm/s)	34.0	11.8	14
Viscosity calculated from Eq. (1) (Pa s)	32.3	92.8	77.1
Settlement of 22 mm Al @ 225 mm	not applicable	35	25
Time (s)		17	15
Average velocity (mm/s)		2.1	1.7
Viscosity calculated from Eq. (1) (Pa s)		62.8	66.4

horizontal dotted lines, in Figs. 5 and 6 are the settlement velocities observed in the tests (see Table 2).

It was observed that both aluminum and steel aggregate settled when the concrete or mortar was vibrated. Applying Eq. (3), it is therefore possible to determine an upper bound for the yield stress of the material. In order for the 19 mm steel sphere to settle in mortar, the yield stress must be less than 50 Pa. Similarly, the yield stress must be less than 5 Pa for the 22 mm aluminum sphere to settle. Since both settled, the yield stress of the vibrated mortar must be less than 5 Pa at all positions from the vibrator where measurements were made. The corresponding yield stress for the concrete is about 4.3 Pa or less. This reinforces the previous conclusions of Tattersall et al. [4,5] and Kakuta and Kojima [8] that vibrated concrete has little or no yield stress.

Table 2 presents the experimentally determined vertical settlement and velocity for each of the tagged spheres. Also shown in Table 2 is the resulting viscosity of the mortar or concrete calculated from Eq. (1). This viscosity value is based on the assumption that under vibration, the mortar and concrete behave as Newtonian fluids, that is, they have zero yield stress. Whether they behave as Newtonian fluids or not, the fact that aluminum spheres of the same size placed at different distances from the vibrator fall at different rates indicates that the rheological properties of the mortar or concrete undergoing vibration depend on the distance from the vibrator. In mortar 1, the viscosity increases from 25.4 Pa s at 75 mm to 32.3 Pa s at 150 mm to 62.8 Pa s at 225 mm. However, the trend is not the same in concrete. The calculated Newtonian viscosity at 150 mm (where the steel sphere settles) is 77.1 Pa s, slightly larger than its value of 66.4 Pa s at 225 mm (where an aluminum sphere settles). It is perhaps possible that the material is not Newtonian throughout. This could be ascertained in future experiments. For example, if the settling velocities of two spheres differing in diameter or density, or both, settling at the same distance from the vibrator results in different calculated Newtonian viscosities, this would indicate that the Newtonian model does not represent well the rheological behavior of the material.

As would be expected for the denser medium, settlement in concrete is less than that in mortar. The experimental results support this conclusion.

5. Conclusions

This paper summarizes a unique method and the results of initial tests using this method of real-time monitoring of aggregate settlement in fresh concrete or mortar. Using a scintillation camera and spheres tagged with a radioactive isotope, it has been demonstrated that real-time images of these spheres settling in vibrated mortar or concrete may be obtained. These images were analyzed and the following conclusions reached.

(1) Without vibration, typically-sized aggregate does not settle in mortar or concrete. Furthermore, settlement stops immediately after vibration is terminated.

(2) Vibration reduces both the yield stress and the viscosity of the mortar or concrete. The yield stress becomes very small and approaches zero when subjected to vibration. This change from the unvibrated state is almost instantaneous.

(3) Although the yield stress approaches zero, the mortar or concrete may continue to behave as a Bingham plastic.

(4) The effect of vibration on the yield stress and the viscosity is more pronounced near the vibrator. This effect extends at least 225 mm from the vibrator.

(5) A tendency for aggregate to migrate horizontally toward the vibrator was observed.

Acknowledgments

The authors acknowledge the invaluable assistance of Dr. Peter Blue, Head of Radiology at Moncrief Hospital on Fort Jackson, Columbia, SC. The authors also wish to thank Graduate Research Assistant Baolin Wan and Undergraduate Research Assistants Mike DeFreese and Bryan Thomas who helped to conduct the scintillation camera experiments.

This study was supported by the South Carolina Department of Transportation.

References

[1] D.D. Double, A. Hellawell, The solidification of cement, Sci Am (237) (July 1977) 82–90.
[2] M.F. Petrou, B. Wan, W.S. Joiner, C.G. Trezos, K.A. Harries, Excessive strand end slip in prestressed piles, ACI Struct J, submitted for publication.
[3] G.H. Tattersall, P.F.G. Banfill, The Rheology of Fresh Concrete, Pitman Advanced Publishing Program, London, 1983.
[4] A.N. Beris, J.A. Tsamopoulos, R.C. Armstrong, R.A. Brown, Creeping motion of a sphere through a Bingham plastic, J Fluid Mech 158 (1985) 219–244.
[5] G.H. Tattersall, P.H. Baker, The effect of vibration on the rheological properties of fresh concrete, Mag Concr Res 40 (13) (June 1988) 79–89.
[6] G.H. Tattersall, Effect of vibration on the rheological properties of fresh cement pastes and concretes, in: P.F.G. Banfill (Ed.), Rheology of Fresh Cement and Concrete, Proceedings of the International Conference, University of Liverpool, UK, March 16–29. Chapman & Hall, London, 1990, pp. 323–338.
[7] F. de Larrard, C. Hu, T. Sedran, J.C. Szitkar, M. Joly, F. Claux, F. Derkx, A new rheometer for soft-to-fluid fresh concrete, ACI Mater J 94 (3) (May–June 1997) 234–243.
[8] S. Kakuta, T. Kojima, Rheology of fresh concrete under vibration, in: P.F.G. Banfill (Ed.), Rheology of Fresh Cement and Concrete, Proceedings of the International Conference, University of Liverpool, UK, March 16–29. Chapman & Hall, London, 1990, pp. 339–342.
[9] C. Hu, F. de Larrard, The rheology of fresh high-performance concrete, Cem Concr Res 26 (2) 1996 283–294.
[10] C.F. Ferraris, F. de Larrard, Testing and Modeling of Fresh Concrete Rheology, NIST Report #NISTIR 6094, Feb. 1998.
[11] J. Szwabowski, Influence of three-phase structure on the yield stress of fresh concrete, in: P.F.G. Banfill (Ed.), Rheology of Fresh Cement and Concrete, Proceedings of the International Conference, University of Liverpool, UK, March 16–29. Chapman & Hall, London, 1990, pp. 241–248.
[12] L. Struble, R. Szecsy, Rheology of fresh concrete, in: K.P. Chong (Ed.), 4th ASCE Materials Eng. Conf. Proc., Materials for the New Millenium, (1996) 1121–1128.
[13] W.G. Lei, L.J. Struble, Microstructure and flow behavior of fresh cement paste, J Am Ceram Soc 80 (8) (1997) 2021–2028.
[14] M.F. Petrou, B. Wan, F. Gadala-Maria, V.G. Kolli, K.A. Harries, The influence of mortar rheology on aggregate settlement, ACI Mater J, submitted for publication.